

# A correlated *ab initio* study of Karplus relations for model peptides

S. Ajith Perera and Rodney J. Bartlett\*

Quantum Theory Project, University of Florida, Gainesville, Florida 32611-8435, USA

Received 26 March 2001; Revised 5 June 2001; Accepted 6 June 2001

The equation-of-motion coupled cluster (EOM-CCSD) method was employed to study the variation of proton–proton NMR spin–spin coupling constants with the dihedral angle for coupled protons while all other bond lengths and angles were allowed to relax. *N*-Methylacetamide was chosen as a frequently studied prototype of substantial experimental interest. The constants (*A*, *B* and *C*) governing the behavior of the coupling constants with the dihedral angle were determined in a fully *ab initio*, correlated manner and were compared with others in the literature. Copyright © 2001 John Wiley & Sons, Ltd.

**KEYWORDS:** NMR; *ab initio*; Karplus relations; peptides; *N*-methylacetamide; hydrogen bonds

## INTRODUCTION

In this issue on NMR pertaining to hydrogen bonds, which have an essential role in the orientation of peptide groups in proteins, we believe that it is useful to demonstrate the role of *ab initio* correlated methods in determining NMR coupling that shed light on the orientation of peptide links, along with our application to the two-bond couplings<sup>1–3</sup> across H-bonds, discussed here and elsewhere. These are complementary applications and illustrative of how predictive quantum chemical methods can be employed to provide information that is difficult to obtain experimentally.

The variation of vicinal NMR spin–spin coupling constants with the dihedral angle between coupled nuclei is a well-known phenomenon<sup>4,5</sup> (see Fig. 1 for an illustration of the dihedral angles of interest). Such variations are assumed to be described by model mathematical relations between the spin–spin coupling constants and the dihedral angle  $\phi$  of the coupled nuclei. Often these relations have the form

$${}^3J = A \cos^2 \phi + B \cos \phi + C \quad (1)$$

commonly known as 'Karplus relations'.<sup>4,6–8</sup> The basic assumption given in Eqn (1) is that the coupling constants are predominantly dependent on the dihedral angle between the coupled nuclei. X-ray crystallographic studies, coupled with high-resolution NMR measurements, have been used to determine such relations,<sup>9–11</sup> typically by studying a series of compounds in similar environments. However, since it is difficult to arrange experimentally a given system in the various conformations that are required for a fully experimental determination, theory has a powerful potential

role in obtaining reliable coupling constant surfaces if it can be 'predictive.'

At present, the most powerful means for studying the structures of polypeptides in solution is NMR spectroscopy, which, in static conformational analysis, does not lag far behind x-ray crystallographic methods. An outstanding merit of the NMR method is its ability to provide insight into dynamical aspects of the three-dimensional molecular structure and intra- and intermolecular interactions in solution. The application of Karplus relations coupled with high-resolution multi-dimensional NMR spectroscopic measurements is beginning to complement other types of investigations of polypeptides in solution. Furthermore, with the new observations now possible for NMR coupling constants across H-bonds,<sup>1–3,12</sup> the potential role for NMR is even greater; and now a complementary predictive theoretical approach is available, offering its additional insight.

Coupling constants are intricate functions of the geometric (bond lengths, angles) and electronic parameters of the molecule under consideration. As shown in several previous theoretical studies,<sup>13–17</sup> at the *ab initio* Hartree–Fock level of theory, there are large error bars in the calculated NMR spin–spin coupling constants, so relations [similar to Eqn (1)] that are derived from the results of these qualitative theoretical calculations must be used with caution, as well as those obtained from using semiempirical methods.<sup>18–20</sup> Until recently there have been no quantitatively accurate, correlated theoretical methods for the reliable calculation of the variation of the coupling constants as a function of molecular parameters in the context of conformational analysis.<sup>21</sup> Others have considered vibrational and thermal corrections.<sup>22,23</sup> In this paper, we present such a study of *N*-methylacetamide (NMA),<sup>24–26</sup> by employing the recently developed equation-of-motion coupled cluster (EOM-CC) approach.<sup>14,15,27,28</sup>

\*Correspondence to: R. J. Bartlett, Quantum Theory Project, University of Florida, Gainesville, Florida 32611-8435, USA.  
E-mail: bartlett@qtp.ufl.edu  
Contract/grant sponsor: United States Air Force Scientific Research; Contract/grant number: F49620-98-1-0116.

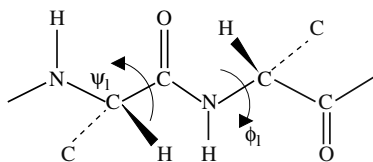


**Figure 1.** Spatial arrangement of a polypeptide chain. The angles  $\phi_1$  and  $\psi_1$  are the dihedral angles of interest.

To obtain  $A$ ,  $B$  and  $C$  in Eqn (1), the most rigorous treatment requires optimization of all the degrees of freedom of the molecule for a given value of the dihedral angle. This feature is very different than conventional estimates made with all bond distances and angles fixed at their equilibrium values. This is conveniently accomplished in the EOM-CCSD method as geometries are optimized at the correlated level for a given value of the dihedral angle. Because of the large amount of experimental and theoretical data available in the literature for comparison, in this initial study we apply the EOM-CCSD<sup>14,15</sup> method to study the variation of the vicinal  $^3J(^1\text{H}, ^1\text{H})$  with the dihedral angle in NMA. The conditions for the determination of the angle  $\phi_l$  (see Fig. 1) by measuring coupling constants are favorable because there is a pair of vicinal protons between which the coupling is large and strongly dependent on  $\phi_l$ . However, the experimental condition for the NMR determination of the angle  $\psi_l$  is less favorable because there is no vicinal proton–proton coupling that can be used for this purpose. Here, our focus is mainly on the variation of the angle  $\phi_l$  for a fixed value of  $\psi_l$ . We take advantage of Edison *et al.*'s findings<sup>9</sup> that the vicinal  $^3J(^1\text{H}, ^1\text{H})$  coupling constant has only a slight dependence on the angle  $\psi_l$ . In addition to NMR spin–spin coupling constants, we consider geometries, energetics and vibrational frequencies of the *cis* and *trans* forms of NMA. We also consider the NMR spin–spin coupling of formamide, which is experimentally known and provides us with useful calibrating information.

## COMPUTATIONAL DETAILS

The geometry of formamide, *N*-methylformamide and *N*-methylacetamide is determined at the CCSD level using a DZP basis set that consists of the (9s,5p,1d)/[4s,2p,1d] contraction for C and O, and the (4s,1p)/[2s,1p] contraction for H. The sp set was taken from Dunning.<sup>29</sup> Polarization exponents were optimized at the correlated level.<sup>30</sup> Both *cis* and *trans* configurations of NMA were considered. We employed the same DZP basis set for the MBPT(2) vibrational frequencies, CCSD single-point energy and EOM-CCSD NMR spin–spin coupling constant calculations at the CCSD/DZP optimized geometries. Spherical harmonic Gaussian basis functions were used in geometry optimization, vibrational frequency calculations and single-point energy calculations. The NMR spin–spin coupling constants were obtained with DZP, DZ (Dunning contraction of sp exponents)<sup>29</sup> and Ahlrichs (qzp, qz2p)<sup>31</sup> basis sets (see also footnotes of Tables 1–4). All the calculations were carried out using the ACES II<sup>32</sup> Program System.

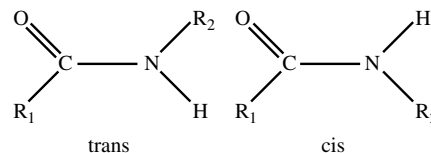


**Figure 2.** The *cis* and *trans* arrangements of a peptide bond.

## RESULTS AND DISCUSSION

Amides provide the simplest models for the structure and conformational characteristics of the backbones of proteins. Formamide is the first in the series. The *cis* and *trans* forms of a generic peptide link are depicted in Fig. 2. The characteristics of the peptide link are the coplanarity of the groups directly attached to it, its partial double bond nature evident from the shorter C–N bond length, substantial rotational barriers (ca 20 kcal mol<sup>-1</sup>) (1 kcal = 4.184 kJ) and preference for the *trans* configuration.<sup>33</sup>

The EOM-CCSD NMR spin–spin coupling constants of formamide and *trans*-*N*-methylformamide are given in Tables 1 and 2, respectively. In the case of formamide, we employed DZP (Basis-I), DZP on heavy atoms and DZ on hydrogens (Basis-II) and qzp on heavy atoms and qz2p on hydrogens (Basis-III) basis sets, whereas *N*-methylformamide calculations were limited to the DZP basis set. As we can see from Table 1, large coupling constants, such as  $^1J(^{15}\text{N}, ^1\text{H})$  and  $^1J(^{13}\text{C}, ^1\text{H})$ , show good agreement with experiment. Also, for such coupling constants, the non-contact contributions are seemingly insignificant. However, as we can see, the proton–proton couplings are relatively small and have large DSO and PSO contributions. Moreover, these non-contact contributions have opposite signs and nearly cancel each other, leaving the FC contribution approximately equal to the total coupling constant. Also, note that the reported coupling constants show only very small variations as we improve the basis set from DZP to Ahlrichs sets, which we have used extensively to obtain very accurate spin–spin coupling constants.<sup>15</sup> As expected, the observed small variations with respect to basis sets are mainly limited to the FC contribution. In other words, the PSO and DSO contributions are insensitive to basis set effects, and one can obtain a very good estimate for these contributions by using basis sets such as DZP on heavy atoms and DZ on hydrogens (Basis-II). Based on these observations, we use Basis-II in NMA calculations, since we are not able to use larger basis sets such as Basis-III owing to the size of the calculation. We can see from Table 1 the EOM-CCSD/Basis-I and also Basis-II and -III results for  $^2J(^1\text{H}_A, ^1\text{H}_B)$ ,  $^3J(^1\text{H}_B, ^1\text{H}_C)$  and  $^3J(^1\text{H}_A, ^1\text{H}_C)$  (including all the non-contact contributions). The latter two are consistently lower than experiment whereas just the FC contributions are both larger and smaller than experiment and less systematic. On average, EOM-CCSD/DZP results for vicinal proton–proton coupling constants in formamide underestimate experiment by about 2 Hz. The EOM-CCSD NMR spin–spin coupling constants of *N*-methylformamide shows similar behavior to those of formamide (see Table 2). The proton–proton coupling in *N*-methylformamide has a similar chemical environment for model peptide proton–proton couplings that are of interest in this study. In

**Table 1.** NMR spin–spin coupling constants of formamide (Hz)<sup>a</sup>

Coupling		FC	SD	PSO	DSO	Total	Exp.
<sup>1</sup> J( <sup>15</sup> N, <sup>1</sup> H <sub>A</sub> )	Basis-I	-82.98	-0.18	-1.63	-0.30	-85.09	
	Basis-II	-84.03	-0.29	-1.70	-0.31	-86.33	±88.0 <sup>b</sup> , 88.3 <sup>c</sup>
	Basis-III	-86.66	-0.30	-1.99	-0.28	-89.23	
<sup>1</sup> J( <sup>15</sup> N, <sup>1</sup> H <sub>B</sub> )	Basis-I	-83.11	-0.22	-1.80	-0.29	-85.42	
	Basis-II	-84.25	-0.32	-1.87	-0.30	-86.74	±92.0 <sup>b</sup> , 90.7 <sup>c</sup>
	Basis-III	-87.36	-0.36	-2.18	-0.26	-90.16	
<sup>2</sup> J( <sup>15</sup> N, <sup>1</sup> H <sub>C</sub> )	Basis-I	-18.54	0.00	0.26	0.15	-18.13	
	Basis-II	-18.78	0.00	0.30	0.14	-18.34	±19.0 <sup>b</sup>
	Basis-III	-18.80	-0.01	0.25	0.15	-18.41	
<sup>1</sup> J( <sup>13</sup> C, <sup>1</sup> H <sub>C</sub> )	Basis-I	173.72	0.17	-0.72	1.07	174.24	
	Basis-II	179.45	0.24	-0.53	1.09	180.25	
	Basis-III	179.11	0.15	-0.45	1.04	179.85	
<sup>2</sup> J( <sup>13</sup> C, <sup>1</sup> H <sub>A</sub> )	Basis-I	-1.20	-0.12	-0.63	-0.62	-2.57	
	Basis-II	-1.57	-0.12	-0.70	-0.61	-3.00	
	Basis-III	-0.93	-0.14	-0.47	-0.63	-2.17	
<sup>2</sup> J( <sup>13</sup> C, <sup>1</sup> H <sub>B</sub> )	Basis-I	5.43	-0.05	-0.60	-0.63	4.15	
	Basis-II	5.59	-0.04	-0.72	-0.62	4.21	
	Basis-III	6.04	-0.08	-0.45	-0.65	4.86	
<sup>1</sup> J( <sup>13</sup> C, <sup>15</sup> N)	Basis-I	-18.30	-0.03	2.75	-0.09	-15.67	
	Basis-II	-17.67	-0.04	2.83	-0.09	-14.97	
	Basis-III	-19.05	-0.01	2.89	-0.09	-16.26	
<sup>2</sup> J( <sup>1</sup> H <sub>A</sub> , <sup>1</sup> H <sub>B</sub> )	Basis-I	3.52	-0.12	4.71	-6.03	2.08	±2.4 <sup>b</sup>
	Basis-II	2.95	-0.06	3.84	-5.95	0.78	
	Basis-III	3.26	-0.02	6.08	-6.15	3.17	
<sup>3</sup> J( <sup>1</sup> H <sub>B</sub> , <sup>1</sup> H <sub>C</sub> )	Basis-I	0.48	0.13	0.27	-0.49	0.39	±2.1 <sup>b</sup>
	Basis-II	0.44	0.14	-0.05	-0.45	0.08	
	Basis-III	0.44	0.15	0.24	-0.51	0.32	
<sup>3</sup> J( <sup>1</sup> H <sub>A</sub> , <sup>1</sup> H <sub>C</sub> )	Basis-I	10.98	-0.04	2.39	-4.04	9.29	±12.9 <sup>b</sup> , 14.6 <sup>c</sup>
	Basis-II	11.43	-0.04	2.08	-4.01	9.46	
	Basis-III	11.07	-0.03	3.35	-4.08	10.31	

<sup>a</sup> Basis-I (DZP), Basis-II (DZP on heavy atoms and DZ on hydrogens) and Basis-III (qzp on heavy atom and qz2p on hydrogens) NMR spin–spin coupling constants at the CCSD/DZP optimized geometry.

<sup>b</sup> Sunners *et al.*<sup>46</sup> Corresponds to measurements on a pure liquid sample.

<sup>c</sup> Marchal and Canet.<sup>47</sup> Corresponds to measurements on a pure liquid sample.

**Table 2.** NMR spin–spin coupling constants of *trans*-*N*-methylformamide (Hz)<sup>a</sup>

Coupling	FC	SD	PSO	DSO	Total	Exp.
<sup>1</sup> J( <sup>15</sup> N, <sup>1</sup> H <sub>A</sub> )	-83.85	-0.18	-1.67	-0.41	-86.11	
<sup>2</sup> J( <sup>15</sup> N, <sup>1</sup> H <sub>B</sub> )	-17.06	0.00	0.34	0.09	-16.63	
<sup>2</sup> J( <sup>15</sup> N, <sup>1</sup> H <sub>C</sub> )	1.42	0.00	0.67	-0.26	1.84	
<sup>2</sup> J( <sup>15</sup> N, <sup>1</sup> H <sub>D,E</sub> )	1.05	0.00	0.09	-0.19	0.95	
<sup>1</sup> J( <sup>13</sup> C, <sup>1</sup> H <sub>B</sub> )	-169.59	0.14	-0.77	1.16	-169.06	
<sup>2</sup> J( <sup>13</sup> C, <sup>1</sup> H <sup>D,E</sup> )	117.41	0.00	0.18	0.64	118.23	
<sup>2</sup> J( <sup>13</sup> C, <sup>2</sup> H <sub>C</sub> )	123.11	0.00	0.13	0.66	123.90	
<sup>2</sup> J( <sup>13</sup> C, <sup>1</sup> H <sub>A</sub> )	0.25	-0.14	-0.77	1.66	-1.18	
<sup>1</sup> J( <sup>13</sup> C, <sup>15</sup> N)	-18.82	-0.05	2.96	-0.11	-15.70	
<sup>2</sup> J( <sup>1</sup> H <sub>A</sub> , <sup>1</sup> H <sub>C</sub> )	6.06	0.24	0.28	-0.14	6.44	
<sup>3</sup> J( <sup>1</sup> H <sub>C</sub> , <sup>1</sup> H <sub>D,E</sub> )	2.48	-0.08	1.89	-2.90	1.39	±5.0 <sup>b</sup>
<sup>2</sup> J( <sup>1</sup> H <sub>C</sub> , <sup>1</sup> H <sub>D,E</sub> )	-14.13	0.31	1.93	-2.56	14.47	
<sup>2</sup> J( <sup>1</sup> H <sub>D</sub> , <sup>1</sup> H <sub>E</sub> )	-9.55	0.31	1.93	-2.58	-9.89	

<sup>a</sup> EOM-CCSD/DZP NMR spin–spin coupling constants at the CCSD/DZP optimized geometries.

<sup>b</sup> LaPlanche and Rogers.<sup>48</sup>

both formamide and *trans*-*N*-methylformamide most of the deviation from experiment can be attributed to the relatively small atomic basis sets.<sup>15</sup> In the following section, we will employ calculated <sup>3</sup>J(H,H) coupling constants of NMA to develop a 'Karplus relation.' Consequently, the accuracy of the EOM-CCSD/DZP proton–proton coupling constants is of primary concern.

The CCSD/DZP optimized geometries of the lowest energy *cis* and *trans* configurations of NMA are given in Table 3 and depicted in Fig. 3(I) and (II), respectively. The bond lengths of the *cis* and *trans* forms of NMA are close to each other while the key bond angles  $\alpha(\text{NC}_2\text{O})$ ,  $\alpha(\text{H}_\text{C}\text{NC}_2)$ ,  $\alpha(\text{C}_3\text{NC}_2)$ ,  $\alpha(\text{H}_\text{B}\text{C}_1\text{C}_2)$  and  $\alpha(\text{H}_\text{D}\text{C}_3\text{N})$  show significant differences. Table 3 also contains experimental bond lengths and angles reported by Kitano *et al.*<sup>34</sup> from electron diffraction measurements. The experimental values for angles  $\alpha(\text{NC}_2\text{O})$  and  $\alpha(\text{C}_3\text{NC}_2)$  are closer to the CCSD/DZP optimized values of the *trans* form and hence it is clear that the experimental results of Kitano *et al.*<sup>34</sup> correspond to the *trans* configuration. The shorter bond length  $r(\text{C}_2\text{N})$  compared to  $r(\text{C}_3\text{N})$  is an indication of the double bond character of the  $\text{C}_2\text{N}$  bond, and is responsible for the larger barrier to internal rotation with respect to the  $\text{C}_2\text{N}$  axis. The CCSD/DZP optimized  $\text{C}_2\text{N}$  bond length is 0.0172 Å longer than the experimental result. The comparatively large difference between the calculated and experimental results is common for multiple bonds and can be improved by incorporating better basis sets and more electron correlation. Changes in angles  $\alpha(\text{C}_1\text{C}_2\text{N})$  and  $\alpha(\text{C}_2\text{NC}_3)$  from 115.4° and 121.1° in the *trans* form to 115.7° and 126.6° in the *cis* form indicate that the principal changes upon rotation to the *cis* form appear to help accommodate

**Table 3.** Geometries of *cis*- and *trans*-*N*-methylacetamide<sup>a</sup>

	<i>trans</i> form (I)	<i>cis</i> form (II)	Exp. <sup>b</sup>
$r(\text{C}_1\text{C}_2)$	1.524	1.524	1.520
$r(\text{C}_2\text{O})$	1.225	1.224	1.224
$r(\text{C}_2\text{N})$	1.369	1.374	1.386
$r(\text{C}_3\text{N})$	1.455	1.453	1.468
$r(\text{NH}_\text{C})$	1.008	1.011	
$r(\text{C}_1\text{H}_\text{A})$	1.098	1.094	
$r(\text{C}_1\text{H}_\text{B})$	1.097	1.099	
$r(\text{C}_2\text{H}_\text{D})$	1.096	1.096	
$r(\text{C}_2\text{H}_\text{E})$	1.098	1.010	
$\alpha(\text{NC}_2\text{O})$	122.1	121.6	121.8
$\alpha(\text{C}_1\text{C}_2\text{O})$	122.5	122.8	
$\alpha(\text{C}_1\text{C}_2\text{N})$	115.4	115.7	115.2
$\alpha(\text{H}_\text{C}\text{NC}_2)$	119.4	114.5	
$\alpha(\text{C}_3\text{NC}_2)$	121.1	126.6	119.6
$\alpha(\text{H}_\text{A}\text{C}_1\text{C}_2)$	108.6	108.4	
$\alpha(\text{H}_\text{B}\text{C}_1\text{C}_2)$	113.2	110.8	
$\alpha(\text{H}_\text{C}\text{C}_3\text{N})$	110.9	108.3	
$\alpha(\text{H}_\text{D}\text{C}_3\text{N})$	108.5	112.1	
$\tau(\text{H}_\text{A}\text{C}_1\text{C}_2\text{H}_\text{B})$	121.4	121.2	
$\tau(\text{H}_\text{D}\text{C}_3\text{NH}_\text{E})$	119.9	118.8	

<sup>a</sup> Bond lengths are in angstroms and bond angles are in degrees. The reported geometries were obtained at the CCSD/DZP level.

<sup>b</sup> Kitano *et al.*<sup>34</sup>

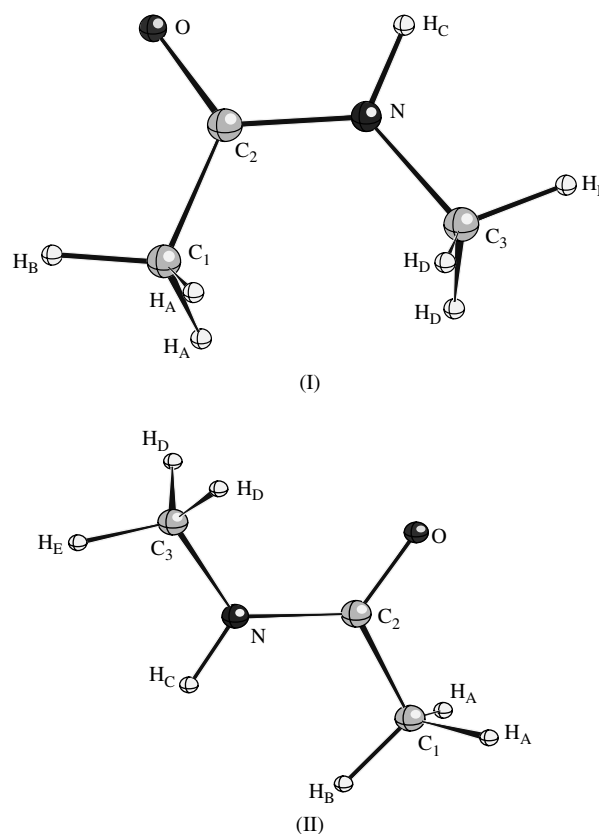


**Figure 3.** CCSD/DZP optimized geometries of *cis* (I) and *trans* (II) forms of NMA (see Table 3 for the values of bond lengths and angles).

the steric congestion. Further evidence for this assertion comes from changes in  $\alpha(\text{H}_\text{C}\text{NC}_2)$  from 119.44° in the *trans* form to 114.45° in the *cis* form. The  $\text{C}_2\text{—N}$  bond length is significantly shorter in the *trans* than the *cis* form.

The stationary points are characterized by vibrational frequency calculations, and the conformations shown in Fig. 3 for the *cis* and *trans* form are actual minima on their respective potential energy surfaces. Vibrational frequencies of the *cis* and *trans* minimum structures [Fig. 3(I) and (II)] are similar and cannot be distinguished from each other by vibrational spectroscopy alone. In the gas phase, the *trans* form [Fig. 3(II)] is 2.30 kcal mol<sup>-1</sup> more stable than the *cis* form [Fig. 3(I)] at the CCSD/DZP level, at the CCSD/DZP geometries. This includes the zero-point energy at 0 K calculated at the MBPT(2)/DZP level. Naturally, the zero-point energy differences are small; the *cis* isomer is favored by 0.026 kcal mol<sup>-1</sup> at the MBPT(2)/DZP level.

Table 4 presents the EOM-CCSD NMR spin–spin coupling constants of the *trans* and *cis* form of NMA. As we have seen from the results for formamide, it is advantageous to include non-contact contributions to have a consistent deviation from experiment. To have a better agreement with experiment requires a basis set better than DZP. For NMA, we are not at liberty to improve upon the atomic basis set beyond DZP. Because of the much greater number of tensor elements, we estimate the DSO and PSO contributions by employing a DZP basis on the heavy atoms and a DZ basis set on hydrogen atoms. As we have concluded in a previous

**Table 4.** NMR spin–spin coupling constants of *cis*- and *trans*-*N*-methylacetamide (Hz)<sup>a</sup>

Coupling	<i>trans</i>	<i>cis</i>	Exp.
$^1J(^{15}\text{N}, ^1\text{H})$	−86.12	−85.90	±93.0 <sup>b</sup>
$^1J(^{15}\text{N}, ^{13}\text{C}_2)$	−15.99	−15.80	
$^1J(^{15}\text{N}, ^{13}\text{C}_3)$	−13.27	−12.67	
$^2J(^{15}\text{N}, ^{13}\text{H}_\text{E})$	0.84	1.47	
$^2J(^{15}\text{N}, ^{13}\text{H}_\text{D})$	1.52	0.89	
$^3J(^{15}\text{N}, ^{13}\text{H}_\text{B})$	−0.47	−2.08	
$^3J(^{15}\text{N}, ^{13}\text{H}_\text{A})$	−1.00	0.39	
$^1J(^{13}\text{C}_1, \text{H}_\text{A})$	116.09	110.68	
$^1J(^{13}\text{C}_1, \text{H}_\text{B})$	111.49	122.86	
$^1J(^{13}\text{C}_3, \text{H}_\text{D})$	127.34	123.74	
$^1J(^{13}\text{C}_3, \text{H}_\text{E})$	116.38	118.19	
$^2J(^1\text{H}_\text{A}, \text{H}_\text{A})$	−17.41	−16.55	
$^2J(^1\text{H}_\text{A}, \text{H}_\text{B})$	−13.57	−13.88	
$^2J(^1\text{H}_\text{D}, \text{H}_\text{D})$	−13.33	−11.12	
$^2J(^1\text{H}_\text{D}, \text{H}_\text{E})$	−13.85	−15.10	
$^3J(^1\text{H}_\text{D}, \text{H}_\text{C})$	1.17	1.55	
$^3J(^1\text{H}_\text{E}, \text{H}_\text{C})$	5.36	6.67	
$^4J(^1\text{H}_\text{A}, \text{H}_\text{C})$	−0.81	−1.34	
$^4J(^1\text{H}_\text{B}, \text{H}_\text{C})$	0.83	0.59	

<sup>a</sup> The FC contributions were calculated using a DZP basis and the PSO and DSO contributions were calculated using a DZP basis on heavy atoms and a DZ basis on hydrogens. The small SD contributions are neglected.

<sup>b</sup> Marchal and Canet.<sup>47,49</sup> Corresponds to measurements on a pure liquid sample.

study<sup>15</sup> and also seen from the calculations on formamide, this will give us a fairly accurate estimate of these two contributions since they are more or less insensitive to the choice of the atomic orbital basis sets.

The calculated coupling constants  $^1J(^{15}\text{N}, ^1\text{H})$  and  $^1J(^{13}\text{C}, ^1\text{H})$ , given in Table 4, are consistent with the literature values for  $sp^2$  hybridized N–H and  $sp^3$  hybridized C–H coupling constants.<sup>35–37</sup> As expected from the similar geometries and bonding character, these coupling constants have similar values in the *cis* and *trans* forms. The multiple-bond character of the  $\text{C}_2$ –N bond is reflected by its relatively large negative value for  $^1J(^{13}\text{C}_2, ^{15}\text{N})$  compared with  $^1J(^{13}\text{C}, ^{15}\text{N})$  in  $\text{CH}_3\text{NH}_2$  and its shorter  $\text{C}_2$ –N bond length compared with the C–N single bond length (ca 1.46). As we have seen earlier, in the *cis* form  $\text{H}_\text{C}$  and  $\text{H}_\text{E}$  are closer in space compared with the corresponding atoms in the *trans* form. This is also reflected in the large  $^3J(^1\text{H}_\text{E}, ^1\text{H}_\text{C})$  value in the *cis* form compared with the *trans* form. Similarly,  $\text{H}_\text{B}$  and  $\text{H}_\text{C}$  are further apart in the *cis* form and have a smaller coupling constant than the *trans* form. Consequently, the relative magnitude of the  $^3J(^1\text{H}, ^1\text{H})$  may be used to assign the configuration (*cis* or *trans*) of the peptide unit.

Several experiments were performed to measure the NMR spectrum of NMA. The *cis* isomer is present in too small a proportion (ca 3% in water) to be observed in the NMR measurements. As a result, experimentally measured NMR chemical shifts and spin–spin coupling constants are

mostly due to the *trans* isomer. The EOM-CCSD/DZP results for the  $^1J(^{15}\text{N}, ^1\text{H})$  coupling constant, when considered with the mean absolute error of such a method as reported previously (ca 12%), are in good agreement with experiment. As indicated on several occasions, the EOM-CCSD results almost always provide an unambiguous determination of the sign of the coupling constant and the  $^1J(^{15}\text{N}, ^1\text{H})$  is, in fact, negative. The long-range  $^3J(^{15}\text{N}, ^1\text{H})$  coupling constant has been reported to be  $\pm 1.63$  Hz,<sup>38</sup> and taking into account the error bars of the EOM-CCSD/DZP level, compares very well with the rotationally averaged calculated result for the *trans* isomer (−0.82 Hz).

We are most interested in  $^3J(^1\text{H}_\text{C}, ^1\text{H}_\text{D,E})$  coupling constants. The calculated  $^3J(^1\text{H}_\text{C}, ^1\text{H}_\text{D,E})$  coupling constant for several different values of the dihedral angle  $\phi$  is given in Table 5. If it is assumed that the hydrogens of the methyl group occupy discrete rotational states with one of the methyl protons *cis* to the NH proton (energetically preferred conformation), then the calculated average  $^3J(^1\text{H}_\text{C}, ^1\text{H}_\text{D,E})$  coupling constants for the *trans* and *cis* forms are 2.6 and 3.3 Hz, respectively. The corresponding experimental values are 4.8 and 5.3 Hz, respectively.<sup>39</sup> This difference of 2 Hz is similar to those shown previously for formamide and *N*-methylformamide. Consequently, it is fair to assume that the calculated results are systematically lower by about 2 Hz for the proton–proton coupling constants of interest in these molecules, so we add 2 Hz to the calculated results to account for basis set limitations. The scaled values are also presented in Table 5 (given in parentheses). The range of  $^3J(^1\text{H}_\text{C}, ^1\text{H}_\text{D,E})$  as the dihedral angle varies from 0 to 180° is 7.36–10.25 Hz in the *trans* form and 8.67–11.31 Hz in the *cis* form. The disadvantage of having such a small range for the  $^3J(^1\text{H}_\text{C}, ^1\text{H}_\text{D,E})$  is that the smaller errors in the calculated or experimentally measured  $^3J(^1\text{H}_\text{C}, ^1\text{H}_\text{D,E})$  will correspond to larger errors in the dihedral angle in question. In other words, to minimize these errors, the calculated  $^3J(^1\text{H}_\text{C}, ^1\text{H}_\text{D,E})$  results for the different dihedral angles that we will employ to estimate *A*, *B* and *C* are required to be highly accurate. The scaled values for the  $^1J(^1\text{H}, ^1\text{H})$  coupling constants for

**Table 5.** Variation of  $^3J(^1\text{H}, ^1\text{H})$  with dihedral angle of *cis* and *trans*-*N*-methylacetamide (Hz)<sup>a</sup>

Dihedral angle (°)	<i>trans</i>	<i>cis</i>
0	5.36 (7.36)	6.67 (8.67)
30	3.96 (5.96)	4.68 (6.68)
60	0.29 (2.29)	0.50 (2.50)
120	1.17 (3.17)	1.55 (3.55)
150	5.52 (7.52)	6.53 (8.53)
180	8.25 (10.25)	9.31 (11.31)

<sup>a</sup> The EOM-CCSD spin–spin coupling constants at the CCSD/DZP optimized geometries. The FC contributions were calculated using a DZP basis and the PSO and DSO contributions were calculated using a DZP basis on heavy atoms and a DZ basis on hydrogens. Small SD contributions are not included. The numbers in parentheses contain a 2 Hz correction (see text for explanation).

different values of the dihedral angle  $\phi$  presented in Table 5 are used to estimate the magnitudes of  $A$ ,  $B$  and  $C$  in Eqn (1). Within the error bars of the statistical fit, the expressions

$${}^3J(\text{H,H}) = (8.09 \pm 0.42) \cos^2 \phi - (1.17 \pm 0.16) \cos \phi + (0.70 \pm 0.31) \quad (2)$$

$${}^3J(\text{H,H}) = (9.27 \pm 0.20) \cos^2 \phi - (1.19 \pm 0.08) \cos \phi + (0.69 \pm 0.15) \quad (3)$$

describe the variations of calculated vicinal  ${}^3J(\text{H,H})$  spin-spin coupling constants with the dihedral angle for the *trans* and *cis* arrangements of the amide bond, respectively. The respective equations are plotted as a function of the dihedral angle  $\phi$  in Figs 4 and 5. In Table 6, we compare the proposed values for the constants  $A$ ,  $B$  and  $C$  with

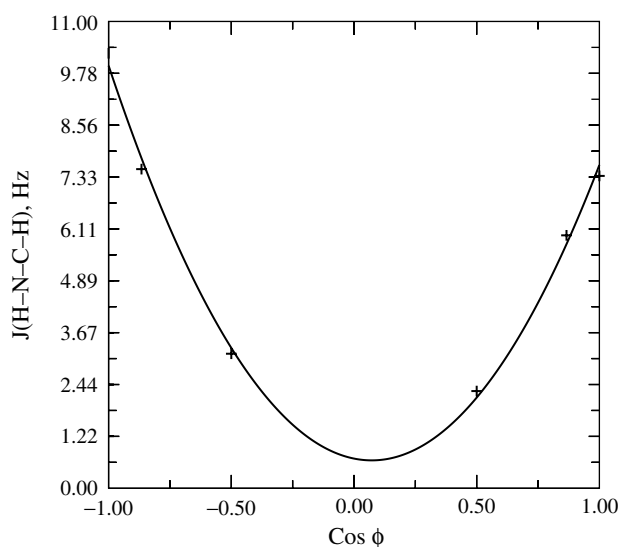


**Figure 4.** Plot of the vicinal  ${}^3J(^1\text{H}, ^1\text{H})$  coupling constant as a function of the dihedral angle for the *trans* arrangement of the amide bond in NMA.

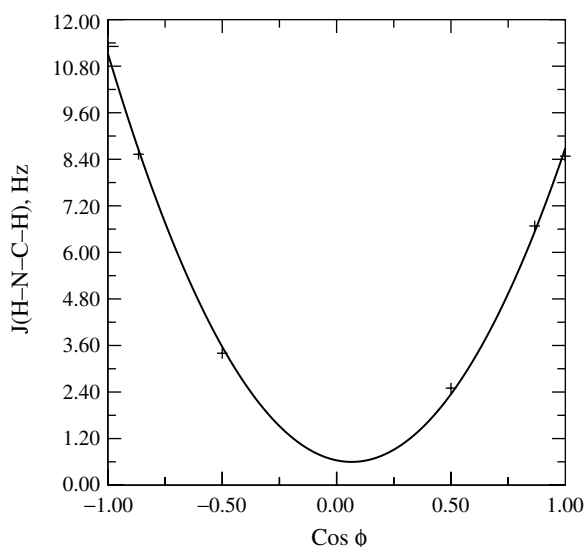


**Figure 5.** Plot of the vicinal  ${}^3J(^1\text{H}, ^1\text{H})$  coupling constant as a function of the dihedral angle for the *cis* arrangement of the amide bond in NMA.

**Table 6.** Coefficients proposed for Eqn 1

Ref.	Configuration	Coefficient (Hz)		
		$A$	$B$	$C$
Bystrov <i>et al.</i> <sup>50</sup>		9.8	1.1	0.4
Néel and co-workers <sup>40,41</sup>		9.3	3.5	0.3
Néel and co-workers <sup>42</sup>		9.4	3.2	0.0
Ramachandran and Chandrasekaran <sup>43</sup>		8.6	1.7	1.5
Barfield and Gearhart <sup>18</sup>	<i>trans</i>	12.06	4.48	0.01
	<i>cis</i>	11.27	4.32	0.01
This work	<i>trans</i>	8.09	1.17	0.70
	<i>cis</i>	9.27	1.19	0.69

several other sets of values reported in the literature. It has been shown that the coefficients proposed by Néel and co-workers<sup>40–42</sup> and Ramachandran and co-workers<sup>43–44</sup> give lower values of  ${}^3J(^1\text{H}, ^1\text{H})$  coupling constants for the *cis*-arranged peptide bonds for the dihedral angles in the range of  $0^\circ \leq \phi \leq 90^\circ$  compared with  ${}^3J(^1\text{H}, ^1\text{H})$  values inferred from the experimentally determined relations.<sup>45</sup> The coefficients proposed by Barfield and Gearhart<sup>18</sup> are based on INDO (intermediate neglect of differential overlap) calculations on the model compound NMA. Contrary to experiment, the relations given by Barfield and Gearhart<sup>18</sup> predict larger  ${}^3J(^1\text{H}, ^1\text{H})$  for the *trans* configuration than that for the *cis* configuration of the amide bond. However, consistent with experiment, the relations derived in this study give larger  ${}^3J(\text{H,H})$  coupling constants for the *cis* arrangement than the *trans* arrangement of the amide bond in the region of  $\phi \approx 0^\circ$ . Our results also predict similar behavior in the region of  $\phi \approx 180^\circ$ . However, it is as yet impossible to verify experimentally that larger  ${}^3J(\text{H,H})$  values for the *cis* than *trans* configuration of the amide bond also hold for this region.

## CONCLUSIONS

We have presented a study of the application of theoretically calculated EOM-CCSD NMR spin-spin coupling constants in conformational analysis. Our focus was the determination of the dihedral angle  $\phi$  (Fig. 1) for NMA by using NMR spin-spin coupling constants.

The structure and energetics of NMA were themselves found to be interesting. The *trans* configuration of the amide bond was shown to be [Fig. 3(II)] 2.30 kcal mol<sup>-1</sup> more stable than the *cis* configuration [Fig. 3(I)] at the CCSD/DZP level, at the CCSD/DZP geometries. The eclipsed conformation of the methyl hydrogens with respect to the N—H and C=O bonds was found to be the most stable conformation for the *cis* configuration of the amide bond. On the other hand, for the *trans* configuration, the eclipsed conformation of the methyl hydrogen with respect to the N—H bond and the staggered conformation with respect to the C=O bond were found to be the most stable conformation. The relative

magnitude of the  ${}^3J(^1\text{H}, ^1\text{H})$  may be useful to assign the configuration of the peptide link.

The relations given in Eqns (2) and (3) for variation of the vicinal coupling  ${}^3J(^1\text{H}, ^1\text{H})$  with dihedral angle for the *trans* and *cis* configurations of the amide bond predict the relative ordering of the  ${}^3J(^1\text{H}, ^1\text{H})$  for the *cis* and *trans* configurations of the amide bond to be consistent with experiment in the region of  $\sim 0^\circ$ . This is a notable improvement over the relations that have been widely used in the literature. However, the absolute accuracy of the dihedral angle  $\phi$  calculated by the given relations needs to be carefully assessed before widespread use of Eqns (2) and (3) in conformational analysis.

Previously, we have emphasized the importance of having very accurate NMR spin–spin coupling constants to develop Karplus relations. We have also been able to demonstrate the difficulties of obtaining accurate spin–spin coupling constants even for small model systems. Therefore, it is essential to find alternative means for improvement, without relying so much on improving the level of theory (i.e. method, basis set, etc.). An alternative way to look at Eqn (1) is that the constants *A* and *B* describe the relative change in spin–spin coupling constants with respect to a base value *C*, with the variation of the dihedral angle. Owing to error cancellations, the relative changes in the NMR spin–spin coupling constants can be calculated accurately. Therefore, the constants *A* and *B* can be estimated fairly accurately by our EOM-CCSD/DZP results. Because the constant *C* is an absolute value, it is difficult to compute accurately from theoretically calculated results. Therefore, we suggest that a better estimate for the constant *C* for a given *A* and *B* may be obtained by using an experimentally measured spin–spin coupling constant for a known dihedral angle, and using the theoretical calculations to describe the changes with  $\phi$ .

As illustrated in this study, the accurate calculations of NMR spin–spin coupling constants of conformers, regardless of the atoms involved, whether or not accessible experimentally, are now possible and should find use in conformational analysis and NMR spectroscopy.

## Acknowledgments

This work was supported by the United States Air Force Scientific Research (Grant No. F49620-98-1-0116) and by a grant of HPC time from the DOD HPC shared Resource Center. We appreciate useful discussions with Dr. Arthur Edison.

## REFERENCES

- Del Bene JE, Bartlett RJ. *J. Am. Chem. Soc.* 2000; **122**: 10480.
- Del Bene JE, Perera SA, Bartlett RJ. *J. Phys. Chem. A* 2001; **105**: 930.
- Del Bene JE, Perera SA, Bartlett RJ. *Magn. Reson. Chem.* **39**: S109–S114.
- Karplus M. *J. Am. Chem. Soc.* 1963; **58**: 2870.
- Marshall JL. *Carbon–Carbon and Carbon–Proton NMR Couplings: Applications to Organic Stereochemistry and Conformational Analysis*. Verlag Chemie International: Deerfield Beach, FL, 1983.
- Karplus M. *J. Phys. Chem.* 1959; **30**: 11.
- Barfield M, Grant DM. *Adv. Magn. Reson.* 1965; **1**: 149.
- Barfield M, Karplus M. *J. Am. Chem. Soc.* 1969; **91**: 1.
- Edison AS, Markley JL, Weinhold F. *J. Biomol. NMR* 1994; **4**: 519.
- Vuister GW, Delaglio F, Bax A. *J. Am. Chem. Soc.* 1992; **114**: 9674.
- Kay LE, Brooks B, Sparks SW, Torchia DA, Bax A. *J. Am. Chem. Soc.* 1989; **111**: 5488.
- Borman S. *Chem. Eng. News* 1999; May10, 36.
- Oddershede J. In *Nuclear Magnetic Resonance. A Specialist Periodical Report*, vol. 19, Webb GA (ed.). Royal Society of Chemistry: Cambridge, 1989; 73–88.
- Perera SA, Sekino H, Bartlett RJ. *J. Chem. Phys.* 1994; **101**: 2186.
- Perera SA, Nooijen M, Bartlett RJ. *J. Chem. Phys.* 1996; **104**: 3290.
- Helgaker T, Jaszunski M, Ruud K. *Chem. Rev.* 1999; **99**: 293.
- Fukui H. *Prog. Nucl. Magn. Reson. Spectrosc.* 1999; **35**: 267.
- Barfield M, Gearhart HL. *J. Am. Chem. Soc.* 1973; **95**: 641.
- Barfield M, Gearhart HL. *Mol. Phys.* 1974; **27**: 899.
- Mohanakrishnan P, Easwaran KRK. *Biopolymers* 1979; **18**: 1769.
- Perera SA. Electron correlation effects on nuclear magnetic resonance spin–spin coupling constant calculations, PhD thesis, University of Florida.
- Wigglesworth RD, Raynes WT, Sauer SPA, Oddershede J. *Mol. Phys.* 1998; **94**: 851.
- Wigglesworth RD, Raynes WT, Kirpekar S, Oddershede J, Sauer SPA. *J. Chem. Phys.* 2000; **112**: 3735.
- Mirkin NG, Krimm S. *J. Mol. Struct.* 1996; **377**: 219.
- Hirst JD, Hirst DM, Brooks CL III. *J. Phys. Chem. A* 1997; **101**: 4821.
- Torii H, Tatsumi T, Kanazawa T, Tasumi M. *J. Phys. Chem. B* 1998; **102**: 309.
- Perera SA, Bartlett RJ, Schleyer PVR. *J. Am. Chem. Soc.* 1995; **117**: 8476.
- Perera SA, Bartlett RJ. *J. Am. Chem. Soc.* 1996; **118**: 7849.
- Dunning TH Jr. *J. Chem. Phys.* 1970; **53**: 2823.
- Redmon LT, Purvis GD III, Bartlett RJ. *J. Am. Chem. Soc.* 1979; **101**: 2856.
- Schäfer A, Horn H, Ahlrichs R. *J. Chem. Phys.* 1992; **97**: 2571.
- ACES II program is a product of Quantum Theory Project, University of Florida. Stanton JF, Gauss J, Watts JD, Nooijen M, Oliphant N, Perera SA, Szalay PG, Lauderdale WJ, Gwaltney SR, Beck S, Balková A, Bernholdt DE, Baeck K-K, Sekino H, Rozyczko P, Huber C, Pittner J, Bartlett RJ. Integral packages included are VMOL (Almlöf J and Taylor P); VPROPS (Taylor PR); a modified version of ABACUS integral derivative package (Helgaker TU, Aa Jensen HJ, Olsen J, Jørgensen P and Taylor PR).
- Schulz GE, Schirman RH. *Principles of Protein Structure*. Springer: New York, 1979.
- Kitano M, Fukuyama T, Kuchitsu K. *Bull. Chem. Soc. Jpn.* 1973; **46**: 384.
- Breitmaier E, Voelter W. *Carbon-13 NMR Spectroscopy*. VCH: New York, 1987.
- Binsch G, Lambert JB, Roberts BW, Roberts JD. *J. Am. Chem. Soc.* 1964; **86**: 5564.
- Bourn AJR, Randall EW. *Mol. Phys.* 1964; **8**: 567.
- Davis DG, Agosta WC, Cowburn D. *J. Am. Chem. Soc.* 1983; **105**: 6189.
- Lier M. *J. Chem. Soc., Perkin Trans. 2* 1972; 720.
- Néel J. *Pure Appl. Chem.* 1972; **31**: 201.
- Cung MT, Marraud M, Néel J. *Ann. Chim. (Paris)* 1972; **7**: 183.
- Cung MT, Marraud M, Néel J. *Macromolecules* 1974; **7**: 606.
- Ramachandran GN, Chandrasekaran R. *Biopolymers* 1971; **10**: 935.
- Ramachandran GN, Chandrasekaran R, Kopple KD. *Biopolymers* 1971; **10**: 2113.
- Bystrov VF. *Pro. Nucl. Magn. Reson. Spectrosc.* 1976; **10**: 41.
- Sunners B, Piette LH, Schneider WG. *Can. J. Chem.* 1960; **38**: 681.
- Marchal JP, Canet D. *J. Am. Chem. Soc.* 1975; **97**: 6581.
- LaPlanche LA, Rogers MT. *J. Am. Chem. Soc.* 1964; **86**: 337.
- Marchal JP, Canet D. *Org. Magn. Reson.* 1981; **15**: 344.
- Bystrov VF, Ivanov VT, Portnova SL, Balashova TA, Ovchinnikov YA. *Tetrahedron* 1973; **29**: 873.